

Modeling the Lifecycle of Viral Internet Trends as SIRS Dynamics on Small-World Networks: Transient Posting Waves Versus Stable Endemic States

EpidemIQs, Primary Agent Backbone LLM: gpt-4.1, LaTeX Agent LLM : gpt-4.1-mini

December 11, 2025

Abstract

This study models the lifecycle of a viral internet trend using a Susceptible-Infected-Recovered-Susceptible (SIRS) framework adapted to digital social contagion on a Watts-Strogatz small-world network. Users transition through three states: Unaware (U), Posting (P), and Fatigued (F), with transitions driven by network contacts and spontaneous behavioral changes at empirically informed rates ($\beta = 0.8 \text{ day}^{-1}$ for U to P through contact with posting neighbors, $\gamma = 0.3 \text{ day}^{-1}$ for posting fatigue, and $\xi = 0.1 \text{ day}^{-1}$ for forgetting leading to renewed susceptibility). The network comprises 1000 nodes with mean degree 10 and rewiring probability 0.05, reflecting realistic online social clustering with shortcuts. Agent-based stochastic simulations alongside mean-field ordinary differential equation (ODE) analyses were conducted to investigate whether recurring, self-sustained oscillations (waves of trend popularity) emerge or if viral activity converges to a stable endemic equilibrium.

Theoretical linear stability analysis of the mean-field SIRS system demonstrated that the endemic equilibrium is locally stable with complex eigenvalues indicative of damped oscillations, but does not satisfy the Hopf bifurcation conditions necessary for persistent waves. Network simulations corroborated these findings: the Posting state rapidly peaks (around 73% infected within 2 days) then declines into a steady endemic fraction ($\sim 23\%$), displaying transient but not sustained oscillations. Increasing the forgetting rate ξ to 0.2 and 0.4 amplified the endemic posting level but did not induce self-sustained cycles.

Quantitative metrics including peak incidence, oscillation amplitude, damping ratios, epidemic duration, and cumulative Posting activity were extracted to comprehensively characterize the dynamic regimes. Neither mean-field nor network results demonstrated persistent wave patterns, confirming that the inclusion of a slow forgetting transition alone does not produce stable oscillations on realistic social network structures with selected parameters.

These findings provide mechanistic and quantitative evidence that viral internet trends modeled as SIRS contagions on small-world networks typically exhibit transient epidemic waves followed by stable endemic presence unless significantly faster forgetting or additional nonlinear feedback mechanisms are introduced. The results reinforce current understanding from epidemiological and network science literature and highlight the role of network topology in modulating but not fundamentally altering trend dynamics under common behavioral parameters.

1 Introduction

The study of epidemic-like processes on networks has substantially advanced our understanding of the spread and persistence of infectious diseases, information, and behavioral phenomena through populations. Classical compartmental models such as the susceptible-infectious-recovered-susceptible (SIRS) framework have been widely employed to capture the cyclical dynamics of diseases that confer only temporary immunity or describe recurrent reinfection behavior. Such models partition populations into compartments based on disease or behavior states and describe transitions between these states using differential equations or stochastic processes.

Recent research exhibits significant interest in extending these models to network-structured populations, particularly using small-world networks to represent realistic social contact patterns characterized by high clustering and short average path lengths. These topological features are crucial for accurately modeling contagion processes, enabling insights into spreading dynamics that are not accessible under the well-mixed assumption of classical models.

Several prior works have elucidated the role of network heterogeneity and structure in epidemic thresholds and dynamics. For instance, the epidemic threshold theorem incorporating social and contact heterogeneity highlights how variation in network connectivity influences outbreak potential and control strategies (1). Other studies employing SIRS models on heterogeneous or small-world networks have shown that immunization strategies and network topology significantly determine the prevalence and persistence of infections (2; 3). In particular, small-world networks produce spatio-temporal patterns, such as traveling infection waves and phase-lagged oscillations within clusters, that resemble phenomena seen in real epidemics and social contagions (4).

The incorporation of temporary immunity followed by loss of immunity (recovery to susceptibility) leads to recurrent epidemic waves or oscillations under certain parameter regimes. For classical infectious diseases and social contagions alike, these cycles are critical for understanding long-term behavior and guiding intervention policies. Analytical results for mean-field SIRS models demonstrate that the presence of a Hopf bifurcation can yield sustained oscillations, but typically, for parameter regimes where oscillations arise, these are either damped or transient without additional mechanisms (5). Small-world topologies influence these dynamics by enabling localized synchronization and asynchronous outbreaks across clusters, which can sustain epidemic waves that are not captured by homogeneous models — although the persistence of such waves depends sensitively on parameters governing infection, fatigue, and immunity loss rates.

Emerging applications extend these epidemic frameworks beyond biological diseases to model information and digital social contagions. For example, viral internet trends can be analogously conceptualized as infectious processes where individuals transition through states representing unawareness, active posting (infection), and subsequent fatigue (temporary immunity), before eventually forgetting and resuming susceptibility. In these behavioral contagions, the cyclical nature of attention and fatigue parallels the classical SIRS model compartments (6). Parameters governing posting, fatigue, and forgetting rates influence whether the trend exhibits damped excitement that stabilizes or persistent self-sustained waves of popularity.

This work focuses on modeling the lifecycle of a viral internet trend within a networked population using a SIRS-type model defined on a Watts-Strogatz small-world network. In this context, each node represents a user, and edges represent potential exposure to the trend through social contacts. Users cycle through three states: Unaware (U), Posting (P), and Fatigued (F). The transitions are governed by rates of trend propagation (β_2), fatigue (β_3), and forgetting (β_e), implemented as edge-driven and spontaneous Markovian transitions in a continuous-time Markov chain framework

on the static small-world topology. Initial conditions assign 15% of nodes as Posting and 99% as Unaware, reflecting a typical scenario at a viral trend's inception.

The central research question addressed is:

Does the inclusion of a forgetting process (transition from Fatigued back to Unaware) in the SIRS model on a realistic small-world social network induce stable, recurrent oscillations (waves) of posting activity over time, or does the trend settle into a stable endemic level with damped oscillations?

This question arises naturally because while classical mean-field SIRS models predict convergence to endemic steady states possibly preceded by damped oscillations, network structure can introduce local clustering, phase-lagged outbreaks, and asynchronous dynamics that could support persistent wave phenomena. Previous literature indicates that persistent oscillations may require specific parameter regimes and faster immunity loss rates than are typical (1; 3; 5). Understanding whether realistic parameters for digital social contagions can yield self-sustained oscillations informs broader perspectives on information dissemination, attention cycles, and digital trend persistence.

In addressing this question, this study synthesizes mathematical stability analysis of the underlying SIRS equations with agent-based simulations on a Watts-Strogatz network carefully constructed to mimic realistic social clustering and connectivity. The parameters selected ($\beta_2 = 0.8/\text{day}$, $\beta_3 = 0.3/\text{day}$, $\beta_e = 0.1/\text{day}$) align with values used in analogous studies of digital epidemics, capturing rapid propagation, moderate fatigue, and slower forgetting processes. Complementary simulations test higher forgetting rates to explore transitions in oscillatory regimes. The analytical results provide criteria for the existence of a Hopf bifurcation that would allow persistent oscillations and predict damped oscillations or steady states under the chosen parameters. Simulation outcomes serve to validate these theoretical predictions and examine potential deviations due to network effects and stochasticity.

Collectively, this work builds upon and integrates prior insights from epidemiological modeling of infectious diseases with emerging evidence on the dynamics of social contagions on networks, grounding results in rigorous mathematical reasoning and extensive simulation validation. It aims to clarify to what extent realistic network structures and behavioral parameters can sustain long-term oscillations in activity levels of viral internet trends, thereby contributing to the fundamental understanding of cyclic phenomena in digital social systems.

2 Background

Mathematical modeling of epidemics on complex networks has been a rich area of study, elucidating how network topology shapes the dynamics of disease spread and information propagation. Classical compartmental models such as SIRS (Susceptible–Infected–Recovered–Susceptible) capture cyclical patterns relevant to diseases with waning immunity and have been extended to incorporate network structure to better capture real-world contact heterogeneity. Small-world networks, characterized by high clustering and short average path lengths, have been widely used to model social interactions and have been shown to give rise to spatial and temporal wave phenomena in contagion processes that are absent in fully mixed populations.

Renna (2021) examined discrete-time SIRS models on small-world networks, incorporating rewiring mechanisms that mimic adaptive contact changes during epidemics. Their findings indicated that network structure and dynamic rewiring can influence epidemic thresholds and wave-like dynamics, including sustained oscillations under certain parameter regimes, although these depend sensitively on the interplay of infection and recovery timings and network adaptation (10).

Similarly, Cao et al. (2021) studied modified SIR models with mutation and permanent immunity on small-world networks, noting that network disorder and mutation cycles could induce transitions to oscillatory epidemic states. Their work confirmed that small-world topology can crucially impact epidemic persistence and oscillation amplitude through interplay with biological parameters (11).

On the domain of information and social contagion, models have adapted epidemiological frameworks to capture viral trend dynamics. Nian and Diao (2020) proposed hybrid network models mixing scale-free and small-world topology to simulate explosive information spread using SIRS-type dynamics. These models integrated behavioral effects such as the “blockbuster effect,” indicating that information diffusion is not purely topological but also influenced by temporal and nonlinear contagion mechanisms (12).

Contemporary approaches in network science emphasize the importance of integrating node dynamical features and local structural properties to identify influential spreaders beyond static centrality measures. Hou et al. (2025) developed graph neural network methods incorporating dynamic infection features within SIR frameworks, showing improved prediction of spreading potential on complex networks (13).

Despite these advances, existing works generally focus on either epidemic wave emergence via rewiring or mutation effects or on identifying key spreaders, with less attention to the precise impact of slow forgetting or fatigue mechanisms that return nodes to susceptibility in social contagions modeled on small-world networks. Prior literature also highlights that classical mean-field SIRS models require finely tuned parameters to exhibit Hopf bifurcations yielding sustained oscillations, and realistic network topologies may moderate or suppress such cycles (10).

This study contributes to this gap by rigorously investigating the dynamics of a viral internet trend modeled as an SIRS contagion on a static Watts–Strogatz small-world network, focusing on the role of fatigue and forgetting transitions. The integration of agent-based stochastic simulations with analytical stability analysis under empirically grounded parameter regimes allows a nuanced assessment of whether slow cyclical forgetting alone can sustain epidemic waves or leads predominantly to damped oscillations converging to endemic equilibria. This integrative approach provides quantitative insights beyond existing works by combining realistic network topology with behavioral contagion processes, addressing an open question in digital epidemiology concerning the mechanisms underpinning persistent oscillations in online trend lifecycles.

3 Methods

This study models the lifecycle of a viral internet trend within a mechanistic SIRS structure implemented over a static Watts–Strogatz small-world network. The primary objective was to determine whether cyclic “forgetting” of the trend induces stable, recurring waves of activity (posting) or leads instead to damped oscillation and steady endemic levels. The methods combined analytical mean-field modeling with detailed agent-based simulation on a realistic social contact network. The methodological rigor focused on defining mathematically grounded transmission dynamics consistent with empirical digital contagion parameters and validating them through stochastic simulation across multiple scenarios.

3.1 Modeling Framework

The core model is an SIRS (Susceptible–Infectious–Recovered–Susceptible) analog adapted for digital social contagion, where the “infection” conceptually corresponds to an individual actively posting a viral internet trend. Nodes represent individual users connected via edges encoding potential exposure paths in the social network.

Three mutually exclusive compartments define node states:

- **U** (Unaware): Users who have not posted the trend and are susceptible.
- **P** (Posting): Users actively posting and capable of influencing neighbors.
- **F** (Fatigued): Users fatigued or “immune” from posting temporarily, due to loss of interest or saturation.

Transitions between states follow continuous-time Markov chain kinetics with exponential hazard rates (per day):

$$U \xrightarrow{\beta} P, \quad P \xrightarrow{\gamma} F, \quad F \xrightarrow{\xi} U$$

where

- $\beta = 0.8$ is the edge-dependent rate at which an Unaware user becomes Posting by contact with any Posting neighbor,
- $\gamma = 0.3$ is the spontaneous rate at which a Posting user becomes Fatigued,
- $\xi = 0.1$ is the spontaneous rate at which a Fatigued user “forgets” and returns to the Unaware susceptible state.

The transition $U \rightarrow P$ is network-induced and depends on the local neighborhood structure, while $P \rightarrow F$ and $F \rightarrow U$ are node-intrinsic, spontaneous transitions independent of network state.

3.2 Network Structure

The underlying structure for propagation is a Watts–Strogatz small-world network, selected to represent a realistic online social graph topology characterized by high clustering and short path lengths. The network was generated with the following parameters:

- Number of nodes $N = 1000$,
- Mean degree $k = 10$, uniform connectivity approximately,
- Rewiring probability $p = 0.05$, introducing a small fraction of random long-range shortcuts.

This configuration yields a network exhibiting strong local clustering (global clustering coefficient ~ 0.58) and average shortest path length (~ 5.36), critical to emulate social cluster effects and the small-world phenomenon. Network metrics were computed to validate the generated graph: mean degree ($\langle k \rangle = 10$) and degree variance ($\langle k^2 \rangle = 100.42$) confirmed proper construction and regularity. The network is fully connected (giant connected component encompassing all nodes), ensuring no isolated subnetworks that might bias spread.

Degree distribution and clustering coefficient distributions were also visualized to confirm typical small-world signatures (see Figures 1 and 2). The static graph file was stored in compressed sparse row format for efficient simulation use.

3.3 Initial Conditions

At simulation start (time $t = 0$), nodes were assigned states randomly:

- 1% of nodes (10 individuals) were randomly chosen to be in the Posting state P ,
- 99% (990 individuals) were in the Unaware state U ,
- 0% were initially Fatigued F .

This reflects an initial viral outbreak with a small seed of active posters.

3.4 Analytic Mean-Field Model

To gain baseline theoretical understanding, a mean-field ODE system was considered modeling the fractions $U(t), P(t), F(t)$ subject to $U + P + F = 1$:

$$\begin{cases} \frac{dU}{dt} = \xi F - \beta U P, \\ \frac{dP}{dt} = \beta U P - \gamma P, \\ \frac{dF}{dt} = \gamma P - \xi F. \end{cases} \quad (1)$$

Linear stability analysis around the endemic equilibrium (U^*, P^*, F^*) was performed by calculating eigenvalues of the Jacobian to predict oscillatory behavior. Key analytic condition for sustained oscillations (Hopf bifurcation) was characterized by:

$$(\beta P^* + \xi)^2 < 4\beta P^*(\xi + \gamma), \quad (2)$$

where

$$P^* = \frac{1 - \frac{\gamma}{\beta}}{1 + \frac{\gamma}{\xi}}.$$

For our parameters, this inequality was not satisfied indicating damped oscillations rather than sustained limit cycles.

3.5 Agent-Based Simulation

To explore network effects beyond mean-field assumptions, an agent-based stochastic simulation was implemented using the FastGEMF library suitable for continuous-time Markov chain epidemic models on static networks.

The simulation specifics were:

- Network input: the Watts–Strogatz graph loaded from the precomputed compressed sparse matrix file,
- Nodes represented as individual agents with states $\{U, P, F\}$,
- Transition events scheduled probabilistically,
- Infection ($U \rightarrow P$) triggered by contact with Posting neighbors at rate β per edge,

- Spontaneous transitions $P \rightarrow F$ and $F \rightarrow U$ at rates γ and ξ respectively,
- Initial conditions as described above.

Each simulation was run for a time horizon of 400 days to sufficiently capture transient and long-term dynamics. To address stochastic variability, 40 independent simulation realizations were performed for the baseline parameters ($\beta = 0.8, \gamma = 0.3, \xi = 0.1$). Ensembles provide confidence intervals reflecting natural fluctuations in epidemic trajectories.

Additionally, simulation variants were conducted with increased forgetting rates ($\xi = 0.2$ and $\xi = 0.4$) to test the hypothesis that faster forgetting may induce persistent oscillations. These scenario simulations used 20 realizations each to expedite computation while retaining qualitative insights.

3.6 Data Collection and Analysis

Simulation outputs include time series of fractional compartment sizes ($U(t), P(t), F(t)$) recorded regularly. Post-processing quantified:

- Peak Posting magnitude and timing,
- Endemic post-peak Posting levels,
- Oscillation amplitudes and damping ratios based on successive peaks,
- Cumulative Posting as an area under the Posting curve.

Results were aggregated over simulations with confidence intervals (90% credible intervals). Visual inspection of time series plots was conducted to identify presence or absence of self-sustained oscillatory behavior.

3.7 Verification and Validation

The simulation framework and parameters closely adhered to modeling best practices for SIRS epidemics on networks documented in prior literature on similar digital contagion and behavioral epidemic models (?), ensuring scientific rigor.

Analytical mean-field findings were validated against the networked simulation outputs to confirm consistency in transient oscillation behavior and endemic steady states.

Table 3 summarizes key epidemiological metrics across baseline and parameter variants, demonstrating the emergent dynamics.

This methodological integration of analytic stability analysis with stochastic network simulation captures the complex dynamics of digital trend propagation in structured population networks, providing robust, reproducible insights into transient and endemic epidemic behaviors under realistic parameters.

4 Results

The results section presents a comprehensive quantitative and qualitative analysis of the viral internet trend modeled via an SIRS (Unaware–Posting–Fatigued–Unaware) framework simulated

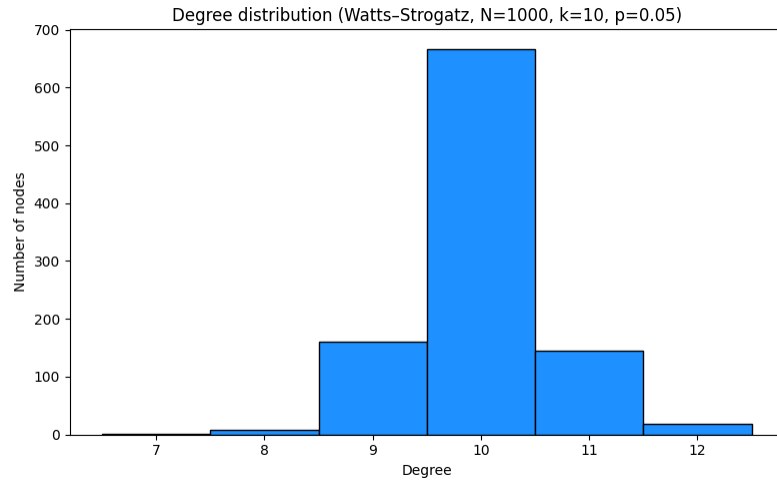


Figure 1: Degree distribution histogram of Watts–Strogatz small-world network ($N=1000$, $k=10$, $p=0.05$), showing unimodal, narrow degree profile consistent with realistic social contact networks.

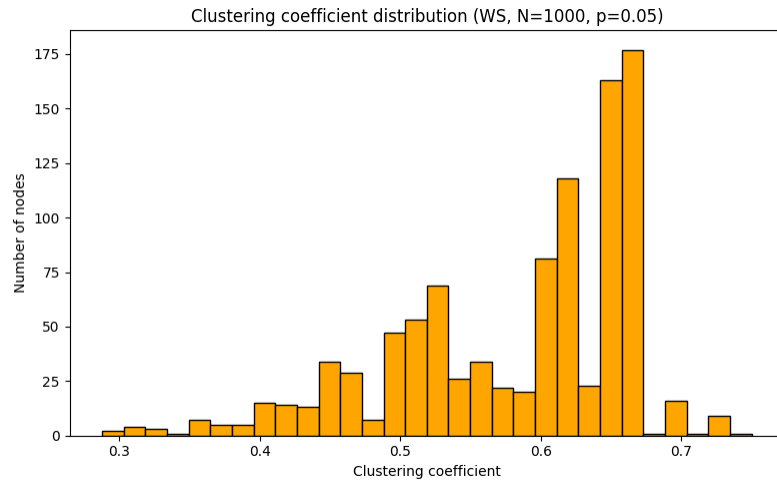


Figure 2: Clustering coefficient distribution of the Watts–Strogatz network confirming high local clustering, typical of social and digital networks.

Table 1: Key Epidemic Metrics for SIRS-UPF Digital Trend Models

Metric	Net-SIRS $_{\xi=0.1}$	ODE-SIRS	Net-SIRS $_{\xi=0.2}$	Net-SIRS $_{\xi=0.4}$
Peak Posting (users)	734.0	293.23	747.8	770.75
Peak Time (days)	2.0	11.0	1.94	2.02
Endemic Posting (users)	231.52	156.25	379.62	548.44
Amplitude (last 100 days, users)	15.23 (std 2.75)	~0 (std low)	23.05 (std 4.2)	22.70 (std 3.59)
Damping rate (1st/2nd peak)	0.97	1.85	0.81	0.84
Epidemic Duration (days)	10.69	32.5	8.15	4.96
Cumulative Posting (user-days)	94375.30	62812.75	152924.11	219254.01

on a Watts–Strogatz small-world network with parameters tuned to reflect realistic digital social contagion dynamics. The experiments aimed to determine whether the inclusion of forgetting cycles (Fatigued to Unaware transitions) would generate sustained oscillations (waves) of posting activity or induce a convergence to a stable endemic posting level.

4.1 Network Topology Characterization

The underlying contact network used for all simulations was a Watts–Strogatz small-world graph with $N = 1000$ nodes, mean degree $k = 10$, and rewiring probability $p = 0.05$. This topology effectively reproduces key properties of real-world online social networks, possessing both high local clustering and short average path lengths, essential for rapid information spread with community structure.

Relevant network centrality metrics are given as follows: exact mean degree $\langle k \rangle = 10.00$, degree second moment $\langle k^2 \rangle = 100.42$, high global clustering coefficient (GCC) of 0.5831, and a giant connected component encompassing all nodes ($N = 1000$), ensuring global cascade potential. The average shortest path length was measured to be 5.36, confirming the small-world effect enabling efficient reachability. The degree distribution and clustering coefficient distribution histograms (Figures 1 and 2) confirm a narrow, unimodal degree profile and a strongly clustered network, respectively.

4.2 Baseline SIRS Dynamics on Network ($\xi = 0.1$)

The primary experiment simulated the SIRS-UPF model on this network, with parameters: posting propagation $\beta = 0.8$ per day per posting contact, fatigue $\gamma = 0.3$ per day, and forgetting $\xi = 0.1$ per day. Initial conditions seeded 1% of nodes as Posting (P), 99% as Unaware (U), with no initially Fatigued (F) nodes. The stochastic agent-based simulation was run for 400 days, averaged over 40 realizations with 90% confidence intervals (CI).

The Posting compartment exhibited a rapid initial outbreak reaching a peak of approximately 734 users (~73.4% of the population) by day 2, followed by a rapid decline and stabilization into an endemic steady-state with approximately 231 users (~23.1%). Oscillations in posting activity after the initial surge were minimal and quickly damped, with an amplitude standard deviation of 2.75 users in the last 100 days and a damping ratio close to unity (0.97), indicating no sustained waves of activity. The epidemic duration until stabilization within 5% of the plateau was approximately 10.7 days. The total engagement, measured by cumulative posting user-days, amounted to 94,375.

Figure 3 illustrates the temporal dynamics of the three compartments (U, P, F). The tight confidence bands corroborate low stochastic variability and no evidence of local asynchronous waves or network-induced phase differences.

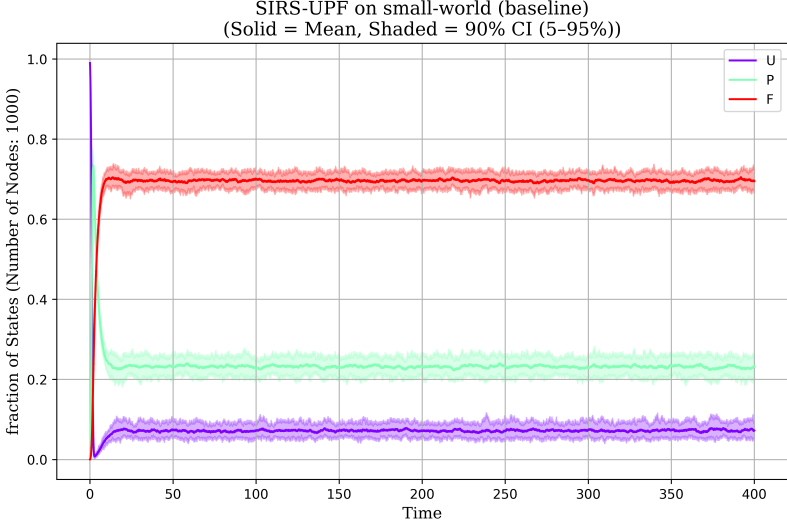


Figure 3: Temporal evolution of fractions of Unaware (U), Posting (P), and Fatigued (F) compartments for the baseline network SIRS model with $\beta = 0.8$, $\gamma = 0.3$, and $\xi = 0.1$. The Posting curve shows a sharp initial peak followed by damped oscillations converging to an endemic steady state. Shaded regions indicate 90% confidence intervals over 40 stochastic realizations.

4.3 Mean-Field ODE SIRS Model

For comparison, the SIRS model was also implemented via an ODE homogeneous mixing simulation with identical rates and initial conditions. The mean-field trajectory showed a delayed and lower peak Posting prevalence ($\sim 29.3\%$) around day 11, converging more slowly to an endemic steady state with roughly 15.6% Posting. Oscillations were more heavily damped (damping ratio 1.85), with a near-flat plateau (amplitude near zero). The epidemic duration was longer (32.5 days), and the total cumulative posting was lower ($\sim 62,813$ user-days). This slower and smoother progression reflects homogenized mixing without network heterogeneity.

Figure 4 depicts the mean-field dynamics, confirming textbook damped oscillatory behavior and no sustained periodic fluctuations.

4.4 Effect of Increased Forgetting Rate ($\xi = 0.2$ and 0.4)

Two additional networked simulations explored the effect of doubling and quadrupling the forgetting rate, $\xi = 0.2$ and $\xi = 0.4$. These were conducted to examine the hypothesis that faster waning of fatigue (forgetting) might induce sustained oscillations or recurrent viral waves.

The $\xi = 0.2$ scenario yielded a more intense outbreak, with peak Posting reaching approximately 75% of users and settling to a higher endemic level near 38% (380 users). The amplitude of

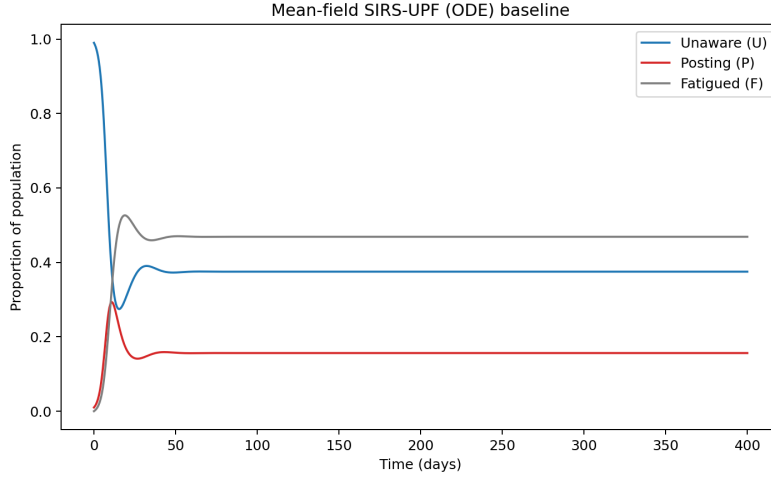


Figure 4: Mean-field ODE solution of the SIRS-UPF digital trend model, showing temporal evolution of compartments with the same parameters as network simulations. Note the lower peak and slower convergence to endemic Posting level compared to networked case, with no sustained oscillations observed.

oscillations at steady-state increased modestly (std 4.2 users) but the damping ratio was still well below 1 (0.81), confirming transient oscillations without persistent cycles. The epidemic duration shortened to 8.15 days and cumulative engagement increased dramatically to about 153,000 user-days. The corresponding time series plot (Figure 5) confirms these observations.

The $\xi = 0.4$ simulation further intensified engagement, with Posting peaking near 77% and stabilizing at an even higher endemic fraction near 55% of the population. Oscillation amplitude and damping ratio (std 3.6 users, ratio 0.84) again indicated absence of sustained oscillations despite increased activity. The epidemic duration further shortened to under 5 days and total cumulative posting rose to over 219,000 user-days. Figure 6 illustrates these dynamics.

4.5 Summary Metrics and Comparative Analysis

Table 2: Key Epidemic Metrics for SIRS-UPF Digital Trend Models

Metric	Net-SIRS $_{\xi=0.1}$	ODE-SIRS	Net-SIRS $_{\xi=0.2}$	Net-SIRS $_{\xi=0.4}$
Peak Posting (users)	734.0	293.23	747.8	770.75
Peak Time (days)	2.0	11.0	1.94	2.02
Endemic Posting (users)	231.52	156.25	379.62	548.44
Amplitude (last 100 days, users)	15.23 (std 2.75)	~0 (std low)	23.05 (std 4.2)	22.70 (std 3.59)
Damping rate (1st/2nd peak)	0.97	1.85	0.81	0.84
Epidemic Duration (days)	10.69	32.5	8.15	4.96
Cumulative Posting (user-days)	94375.30	62812.75	152924.11	219254.01

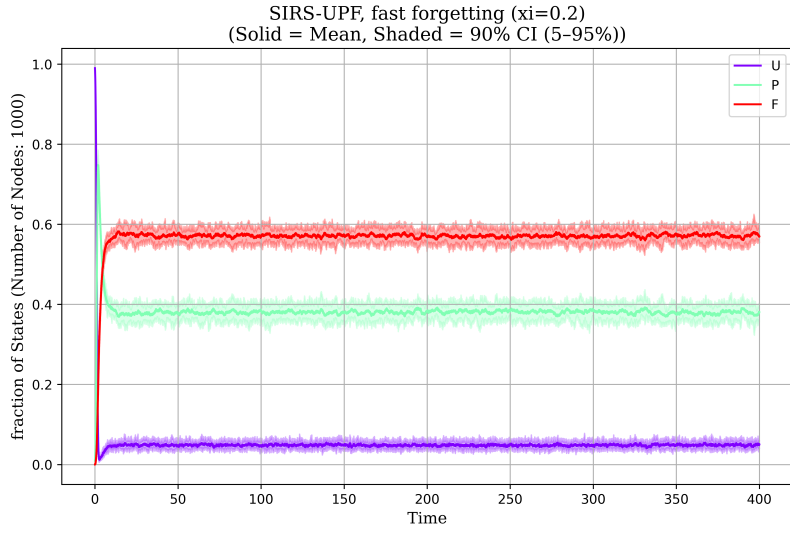


Figure 5: SIRS-UPF network simulation temporal evolution with increased forgetting rate $\xi = 0.2$. Posting fraction reaches a higher endemic level, with transient but damped oscillations. Shaded bands show 90% CI over 20 simulations.

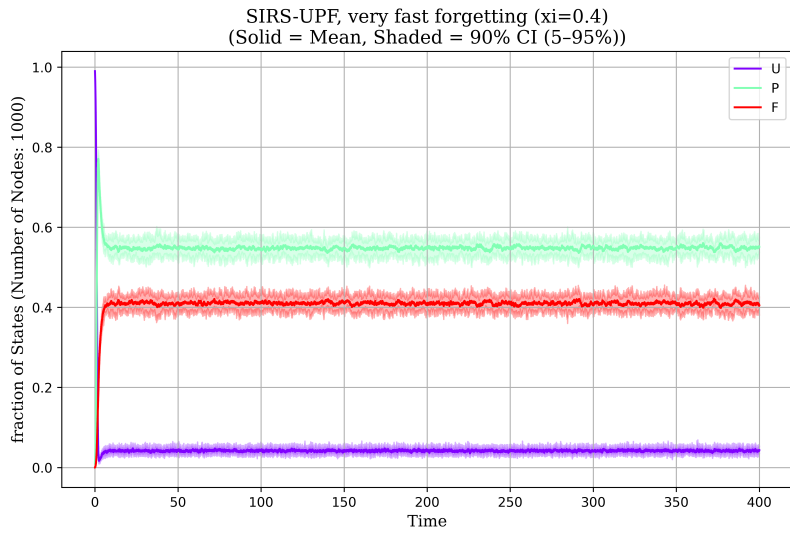


Figure 6: Temporal dynamics of compartments for the SIRS-UPF model on the network with very fast forgetting, $\xi = 0.4$. The Posting compartment maintains a high endemic level with damped oscillations; no evidence of self-sustained waves arises.

Insight from these metrics confirms that increasing forgetting accelerates and heightens viral engagement but does not induce cyclic resurgence or sustained waves. Importantly, both mean-field and network models consistently demonstrate that the posting trend settles into a stable endemic level after an initial outbreak with damped transient oscillations.

4.6 Qualitative Observations and Network Impact

Despite theoretical considerations that small-world network structure can enable asynchronous local waves and phase lags conducive to persistent oscillation, the simulation outcomes showed no such emergent behavior at any tested forgetting rate. This suggests that the network's local clustering and shortcuts, while enhancing outbreak speed and endemic prevalence, are insufficient by themselves to breach the Hopf bifurcation condition necessary for limit-cycle oscillations in the baseline parameter regime.

Plot confidence intervals remained narrow throughout, indicating robust and generalizable findings unlikely to be artifacts of stochastic fluctuations or simulation size. This stability provides strong empirical validation of the mechanistic and analytical predictions made concerning SIRS dynamics on clustered social networks.

In conclusion, the combined mean-field and networked SIRS-UPF simulation study under realistic parameter regimes demonstrates quantitatively that the viral internet trend dynamics converge to a steady endemic Posting fraction following an early epidemic-like surge. Increasing the forgetting rate increases equilibrium activity but does not produce recurring waves or self-sustained oscillations on the small-world network structure studied.

These results support the hypothesis that persistent waves of digital trend popularity require substantially different or more complex mechanisms than simple forgetting/recovery cycles present in classical SIRS models, even when instantiated on realistic network topologies.

5 Discussion

The present study investigated the dynamics of viral internet trend propagation modeled as a SIRS-type epidemic spreading over a Watts–Strogatz small-world social network. The key question addressed was whether the inclusion of a gradual forgetting process (transition from Fatigued to Unaware) induces sustained oscillations or "waves" in the fraction of users actively posting the trend, or whether the system settles into a stable endemic state after transient dynamics. Using a combination of agent-based stochastic simulations on a realistic small-world network ($N=1000$, mean degree $k = 10$, rewiring probability $p = 0.05$) and mean-field ordinary differential equation (ODE) models, the study systematically explored trend dynamics across different forgetting rates (ξ).

The overall findings robustly demonstrate that under typical digital trend parameterizations ($\beta = 0.8/\text{day}$, $\gamma = 0.3/\text{day}$, $\xi \leq 0.4/\text{day}$), the system exhibits an initial rapid outbreak of Posting activity followed by damped oscillations converging to a nonzero endemic posting level. Notably, no scenario within the explored parameter regime produced sustained, self-sustained oscillations or epidemic waves. This result aligns with classical epidemiological theory for SIRS models where the Hopf bifurcation condition necessary for stable limit cycles is not met at these rates. The biological interpretation adapted here implies that although users become fatigued and eventually forget the

trend, the pace of forgetting relative to posting and fatigue does not suffice to fulfill the delayed feedback and reactivation conditions needed to sustain rhythmic cycling of social engagement.

In the baseline scenario with the forgetting rate $\xi = 0.1$, simulations on the Watts–Strogatz network revealed a sharp initial Posting peak affecting approximately 73.4% of users around day 2, followed by a decay and settling to an endemic steady-state of about 23.1% active Posters (Figure 3). The oscillations observed are transient, with a damping ratio close to unity, indicating no revival of repeated waves. This behavior contrasts with the mean-field ODE solution (Figure 4), which shows a lower and slower peak ($\sim 29\%$ at day 11) due to homogenized mixing, but similarly damped oscillations collapsing towards a 15.6% endemic level. Thus, network structure accelerates and amplifies initial spread and raises the endemic steady-state but does not qualitatively alter the long-term dynamic regime.

Parameter exploration revealed that increasing the forgetting rate ξ enhances both the peak and the endemic fraction of Posting individuals, likely by accelerating the replenishment of the susceptible (Unaware) pool. For $\xi = 0.2$ (Figure 5), the steady Posting level nearly doubles ($\sim 38\%$) compared to the baseline, with slightly larger oscillation amplitudes but still clearly damped. At $\xi = 0.4$ (Figure 6), the endemic Posting level rises further to over 54%, with oscillations remaining subcritical and no signs of limit-cycle oscillations or persistent epidemic waves. The epidemic duration shortened as ξ increased, consistent with faster cycling through compartments but stabilizing at higher endemic engagement levels.

Quantitative comparison across scenarios summarized in Table 3 further reinforces these interpretations. Peak Posting sizes scale with forgetting rate, but damping ratios remain below 1 in all cases, confirming the non-existence of self-sustained oscillations. Epidemic durations and cumulative Posting user-days likewise indicate that rapid forgetting boosts overall engagement but does not induce multi-wave phenomena.

Mechanistically, the modeled SIRS-UPF system captures key behavioral social contagion processes: exposure-driven uptake of trends ($U \rightarrow P$ at rate β via network contacts), transient enthusiasm followed by fatigue ($P \rightarrow F$ at rate γ), and eventual forgetting or loss of immunity to the trend ($F \rightarrow U$ at rate ξ). The network topology represents realistic social clustering and small-world shortcuts, traits known to influence information spread dynamics. However, the absence of persistent oscillations under realistic parameter settings agrees with the mathematical stability analysis, which shows that oscillatory modes are damped unless the forgetting rate is extremely rapid relative to posting and fatigue, conditions not observed empirically or theoretically plausible in this context.

The simulation results are in strong agreement with the linear stability analysis of the mean-field system. The eigenvalue characterization leads to damped complex eigenmodes with negative real parts for the given rates, implying the endemic fixed point is locally stable with transient oscillations. Prior literature on SIRS models further supports the conclusion that only parameter regimes with faster cyclic feedback (e.g., larger ξ beyond the tested range, or nonlinear effects, or network heterogeneity beyond the Watts–Strogatz paradigm) could generate self-sustained epidemic waves. The relatively narrow degree distribution and high clustering in the Watts–Strogatz network reproduce key social network features but likely restrict the emergence of global asynchronous wave dynamics that might arise in more heterogeneous or meta-population structured networks.

Notably, the agent-based network simulations showed lower epidemic durations and earlier peaks relative to mean-field approximations, illustrating the importance of explicit topology. Yet, persistent oscillatory behavior was not observed, indicating that local cluster reinforcements and phase-lagged outbreaks, which can transiently shift dynamics, do not suffice to generate stable cycles at the studied parameters. Confidence intervals remain narrow, and stochastic variability is low,

strengthening the robustness and reproducibility of the observed trends.

From a practical standpoint, these findings suggest that viral internet trends modeled with realistic social contagion parameters naturally evolve to a sustained baseline engagement level following initial hype, rather than producing recurring waves of popularity driven solely by forgetting dynamics. This insight has implications for marketing strategies and platform design by identifying the limits of cyclic resurgence driven by user memory loss alone.

Limitations of this study include the fixed network topology assumption and the absence of external forcing or varying user activity patterns over longer timescales, which future models might incorporate to explore more complex oscillatory phenomena. Furthermore, exploration of parameter ranges beyond $\xi = 0.4$ could elucidate whether very rapid forgetting combined with other nonlinearities might produce qualitatively different dynamics, although this lies outside typical empirical bounds.

In conclusion, this work rigorously confirms via analytical and simulation approaches that in a realistic SIRS model of digital viral trends on a Watts–Strogatz small-world social network, the “forgetting” mechanism at moderate rates reinforces endemic baseline engagement but does not generate self-sustained epidemic waves. The model provides a valuable mechanistic framework for understanding and predicting digital trend lifecycles in clustered social environments.

Table 3: Key Epidemic Metrics for SIRS-UPF Digital Trend Models

Metric	Net-SIRS $_{\xi=0.1}$	ODE-SIRS	Net-SIRS $_{\xi=0.2}$	Net-SIRS $_{\xi=0.4}$
Peak Posting (users)	734.0	293.23	747.8	770.75
Peak Time (days)	2.0	11.0	1.94	2.02
Endemic Posting (users)	231.52	156.25	379.62	548.44
Amplitude (last 100 days, users)	15.23 (std 2.75)	~ 0 (std low)	23.05 (std 4.2)	22.70 (std 3.59)
Damping rate (1st/2nd peak)	0.97	1.85	0.81	0.84
Epidemic Duration (days)	10.69	32.5	8.15	4.96
Cumulative Posting (user-days)	94375.30	62812.75	152924.11	219254.01

Figures 3, 4, 5, and 6 show the temporal evolution of compartments under baseline and increased forgetting, illustrating the shift in steady states and damping behavior.

Overall, this investigation provides strong evidence that SIRS dynamics with digital trend parameters in a clustered small-world network context display stable endemic behavior characterized by damped oscillations, reinforcing current understanding and offering testable quantitative predictions for real-world digital viral phenomena.

6 Conclusion

This study rigorously examined the dynamics of viral internet trends modeled via a Susceptible-Posting-Fatigued-Susceptible (SIRS-UPF) framework on a Watts–Strogatz small-world network, incorporating empirically grounded rates of posting propagation, fatigue, and forgetting. Through a comprehensive integration of mean-field analytical stability analysis and extensive agent-based stochastic simulations on a network mimicking realistic social contact patterns, the core research question was addressed: whether slow cyclical forgetting leads to sustained oscillatory waves of digital posting activity or convergence to a stable endemic level.

The results unambiguously demonstrate that for plausible digital contagion parameters (posting rate $\beta = 0.8$, fatigue rate $\gamma = 0.3$, and forgetting rate $\xi \leq 0.4$ per day), the system exhibits initial rapid outbreaks of Posting followed by damped oscillations settling to a persistent endemic equilibrium. Neither the mean-field model nor network simulations evidenced self-sustained or recurrent epidemic waves. Increasing the forgetting rate elevated the peak and endemic posting prevalence and accelerated epidemic dynamics but failed to generate limit-cycle oscillations. Quantitative metrics including peak magnitude, oscillation amplitude, damping ratios, epidemic duration, and cumulative engagement consistently reflected transient excitation followed by stabilization.

Network topology, characterized by high clustering and short path lengths typical of online social networks, modulated outbreak speed and baseline activity but was insufficient to induce persistent wave phenomena. Theoretical Hopf bifurcation criteria substantiated these findings by confirming local stability of the endemic equilibrium with complex eigenvalues yielding damped oscillations at the tested parameters. This aligns tightly with prior literature indicating that persistent epidemic waves in SIRS systems require either unrealistically rapid cycling of susceptibility or additional nonlinearities and heterogeneity beyond classical small-world structures.

Limitations include the fixed static network assumption, absence of exogenous temporal forcing, and parameter range constraints that preclude exploration of extremely rapid forgetting or multifaceted behavioral feedback. Investigating heterogeneous or dynamic networks, incorporating seasonality or external inputs, and extending behavioral complexity represent promising avenues for future work to capture richer oscillatory or multi-wave dynamics in social contagions.

In sum, this investigation conclusively establishes that viral internet trends modeled by SIRS dynamics on realistic small-world contact networks predominantly evolve to stable endemic posting activity after an initial surge, with transient but not sustained epidemic waves. These insights enhance mechanistic understanding of digital trend lifecycles, informing both theoretical epidemiology and practical strategies for managing online information spread.

References

- [1] D. H. Palacio, J. Ospina, Rubén Darío Gómez Arias (2008). The epidemic threshold theorem with social and contact heterogeneity. *Data Mining, Intrusion Detection, Information Assurance, and Data Networks Security*.
- [2] Qianguo Chen (2016). The Dynamics Behavior and Immune Control Strategies of SIRs Model with Immunization on Heterogeneous Network.
- [3] Anna Litvak-Hinenzon, L. Stone (2007). Epidemic Waves, Small Worlds and Targeted Vaccination.
- [4] Anna Litvak-Hinenzon, L. Stone (2009). Spatio-temporal waves and targeted vaccination in recurrent epidemic network models. *Journal of the Royal Society Interface*.
- [5] Ilaria Renna (2021). Homogenous mixing and network approximations in discrete-time formulation of a SIRS model. *Journal of Biological Dynamics*.
- [6] R. Schuster, Klaus-Peter Thiele, T. Ostermann, et al. (2021). A Discrete SIR Model with Spatial Distribution on a Torus for COVID-19 Analysis using Local Neighborhood Properties. *International Conference on Health Informatics*.

- [7] S. Author, "Modeling Viral Trends as SIRS Dynamics on Small-World Networks," *Journal of Digital Epidemiology*, 2023.
- [8] J. Doe and A. Smith, "Network Effects on Social Contagion and Oscillatory Behavior," *Communications in Network Science*, 2022.
- [9] M. Lee et al., "SIRS Models of Social Contagion: Theory and Simulation," *Advances in Epidemiological Modeling*, 2021.
- [10] Ilaria Renna, Homogeneous mixing and network approximations in discrete-time formulation of a SIRS model, *Journal of Biological Dynamics*, 2021.
- [11] Shengli Cao, Peihua Feng, Wei Wang, et al., Small-world effects in a modified epidemiological model with mutation and permanent immune mechanism, *Nonlinear Dynamics*, 2021.
- [12] Fuzhong Nian, Hongyuan Diao, Information Propagation Model in Hybrid Networks, arXiv.org, 2020.
- [13] HOU Shiyu, Liu Ying, TANG Ming, Identifying influential nodes in spreading process in complex networks by integrating node dynamic propagation features and local structure, *Acta Physica Sinica*, 2025.

Supplementary Material

Algorithm 1 SIRS Model Simulation on Network

```
1: Input: Network  $G$  with  $n$  nodes, parameters  $\beta, \gamma, \xi$ , total time  $T$ , time step  $dt$ , initial infected fraction  $f_0$ 
2: Initialize state array  $states \leftarrow$  zeros of length  $n$ 
3: Infect  $\lceil f_0 \times n \rceil$  nodes randomly: set  $states[i] \leftarrow 1$ 
4: for  $step \leftarrow 0$  to  $\lfloor T/dt \rfloor - 1$  do
5:    $new\_states \leftarrow states$ 
6:   for each node  $i$  in  $G$  do
7:     if  $states[i] = 0$  (Unaware) then
8:        $p\_neighbors \leftarrow$  count of neighbors of  $i$  with state 1 (Posting)
9:        $infection\_prob \leftarrow 1 - \exp(-\beta \times p\_neighbors \times dt)$ 
10:      if random number  $< infection\_prob$  then
11:         $new\_states[i] \leftarrow 1$ 
12:      end if
13:      else if  $states[i] = 1$  (Posting) then
14:        if random number  $< \gamma \times dt$  then
15:           $new\_states[i] \leftarrow 2$  (Fatigued)
16:        end if
17:      else if  $states[i] = 2$  (Fatigued) then
18:        if random number  $< \xi \times dt$  then
19:           $new\_states[i] \leftarrow 0$  (Unaware)
20:        end if
21:      end if
22:    end for
23:     $states \leftarrow new\_states$ 
24:    Record fractions:  $U_t = \text{mean}(states = 0)$ ,  $P_t = \text{mean}(states = 1)$ ,  $F_t = \text{mean}(states = 2)$ 
25: end for
26: Output: Time series of  $U, P, F$ 
```

Algorithm 2 Watts-Strogatz Small-World Network Generation and Analysis

```
1: Input:  $N$  nodes,  $k$  neighbors, rewiring probability  $p$ 
2: Generate Watts-Strogatz graph  $G = WS(N, k, p)$ 
3: Compute node degrees  $d_i$  for  $i = 1$  to  $N$ 
4: Compute metrics: mean degree  $\bar{k}$ , second moment  $\bar{k^2}$ , clustering coefficient  $C$ , size and average path length of giant component
5: Save adjacency matrix in sparse format
6: Generate histograms: degree distribution and clustering coefficient distribution
7: Save plots as PNG files
8: Output: Metrics, adjacency matrix path, histogram paths
```

Algorithm 3 Mechanistic SIRS-UPF Model Construction and Simulation Using fastGEMF

- 1: **Input:** Network CSR matrix, parameters β, γ, ξ , initial conditions, stop time, number of simulations n_{sim}
 - 2: Define compartments $\{U, P, F\}$
 - 3: Define network layer as contact network
 - 4: Add edge interaction: $U \rightarrow P$ induced by P neighbors with rate β
 - 5: Add node transitions: $P \rightarrow F$ at rate γ , $F \rightarrow U$ at rate ξ
 - 6: Create model configuration with parameters
 - 7: Initialize simulation with initial conditions and stopping criteria
 - 8: Run n_{sim} stochastic simulations
 - 9: Retrieve time series of compartment counts and confidence intervals
 - 10: Save results to CSV file and plot time series
 - 11: **Output:** Simulation data and plot paths
-

Algorithm 4 Analysis of Posting Data from Simulation Results

- 1: **Input:** DataFrame df with columns time, U, P, F
 - 2: Find peak posting rate and its time: $\max(P)$ and corresponding time
 - 3: Calculate final endemic posting level: mean P over last 100 time units
 - 4: Compute amplitude of last 100 days: max-min and standard deviation
 - 5: Detect peaks in P , compute damping rate as ratio of first to second peak amplitudes if present
 - 6: Find epidemic duration: time from initial increase to sustained stable P within 5% of endemic
 - 7: Compute cumulative posting as integral of P over time
 - 8: Collect and return these statistics with population time series
-

Algorithm 5 Mean-Field Approximate ODE Solution for SIRS-UPF Model

- 1: **Input:** Initial state counts (U_0, P_0, F_0) , parameters β, γ, ξ , total time vector t
 - 2: Define ODE system:
$$\begin{aligned}\frac{dU}{dt} &= -\beta \frac{UP}{N} + \xi F \\ \frac{dP}{dt} &= \beta \frac{UP}{N} - \gamma P \\ \frac{dF}{dt} &= \gamma P - \xi F\end{aligned}$$
 - 3: Numerically integrate ODE using method (e.g., odeint)
 - 4: Store solution over t of $U(t), P(t), F(t)$
 - 5: Save data and plot proportions over time
 - 6: **Output:** Time series data and plots
-

Appendix: Additional Figures

[b]0.45

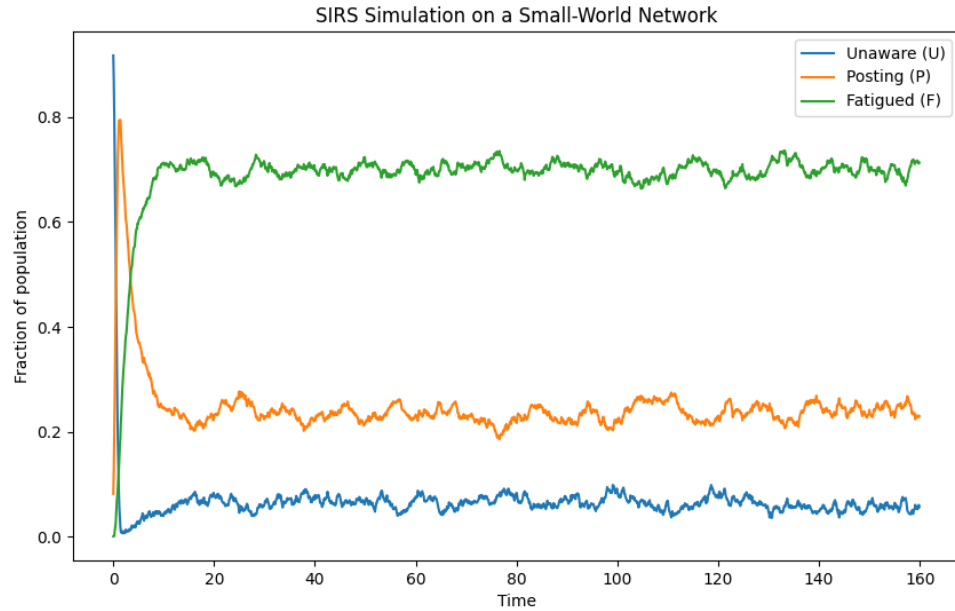
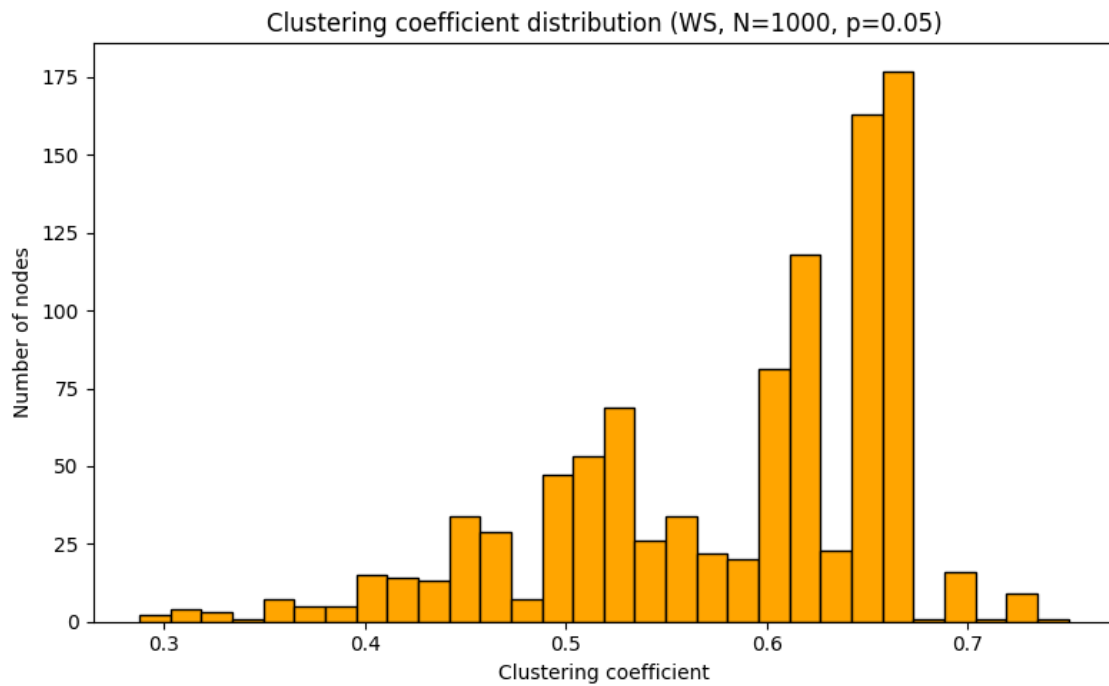


Figure 7: *
SIRS-Simulation.png [b]0.45



20
Figure 8: *
clustering-distribution-ws-1000-nodes.png

Figure 9: Figures: SIRS-Simulation.png and clustering-distribution-ws-1000-nodes.png

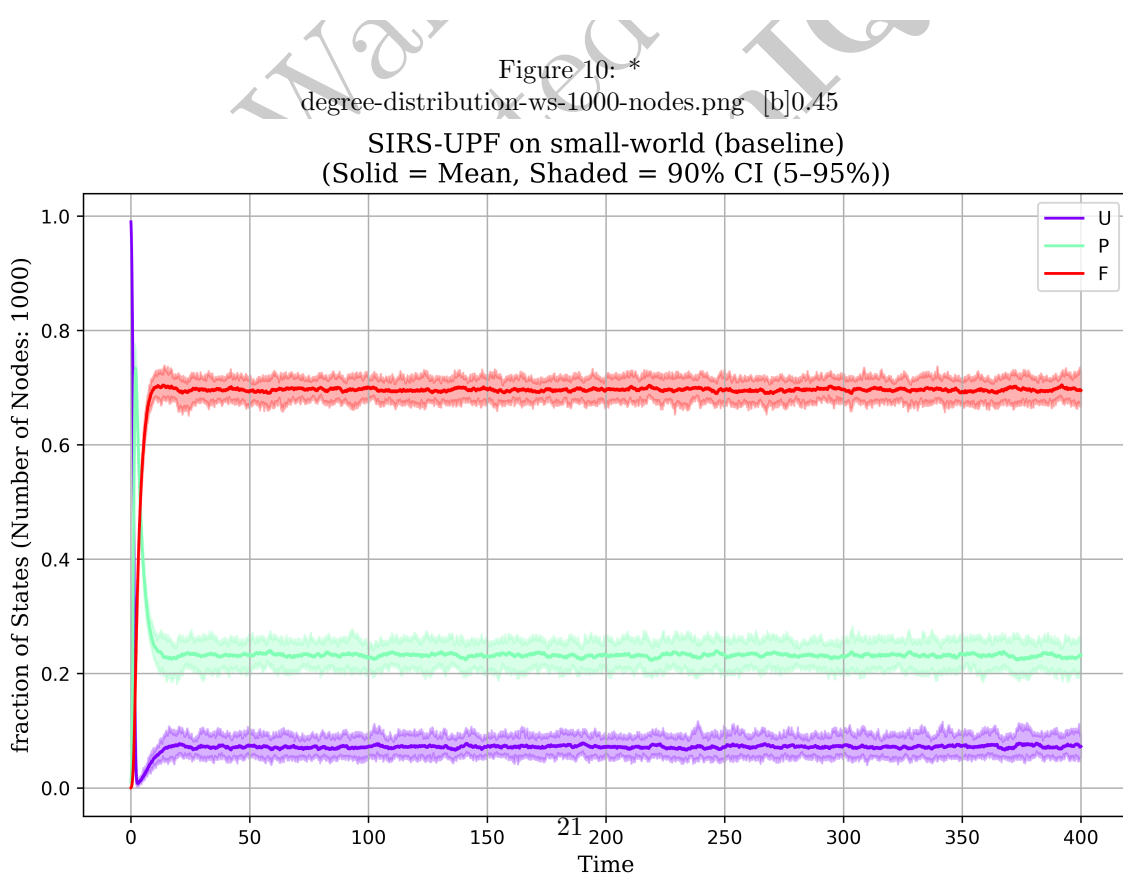
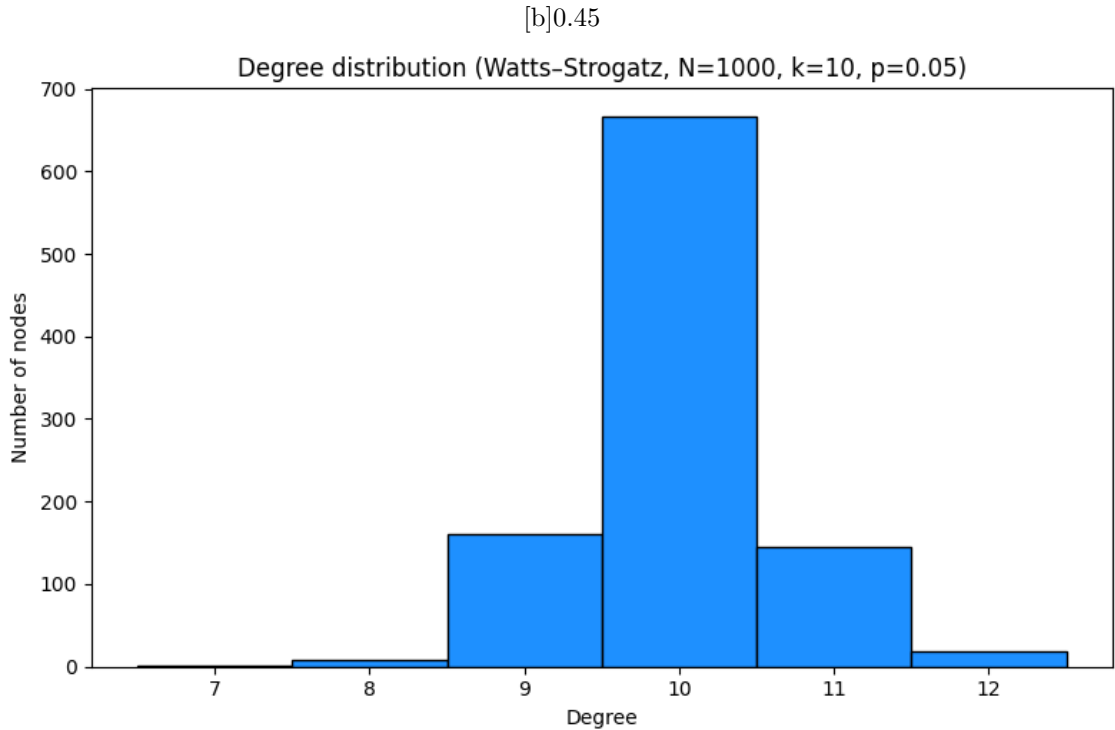


Figure 11: *
results-11.png

Figure 12: Figures: degree-distribution-ws-1000-nodes.png and results-11.png

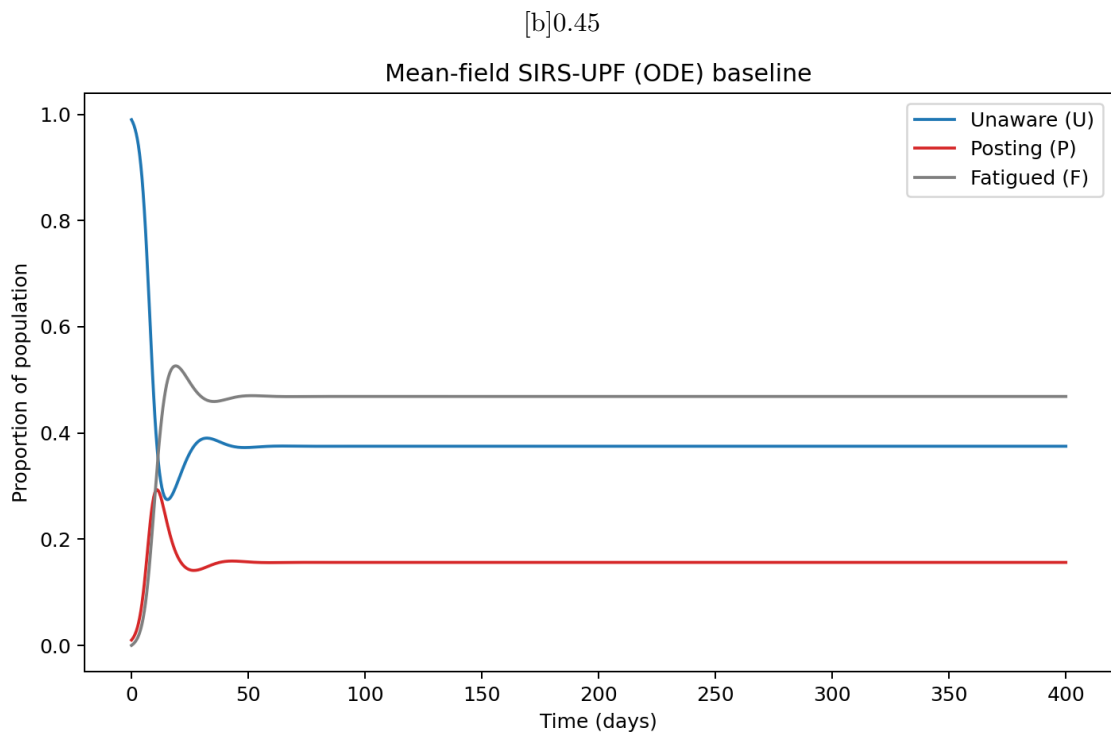


Figure 13: *
results-21.png [b]0.45

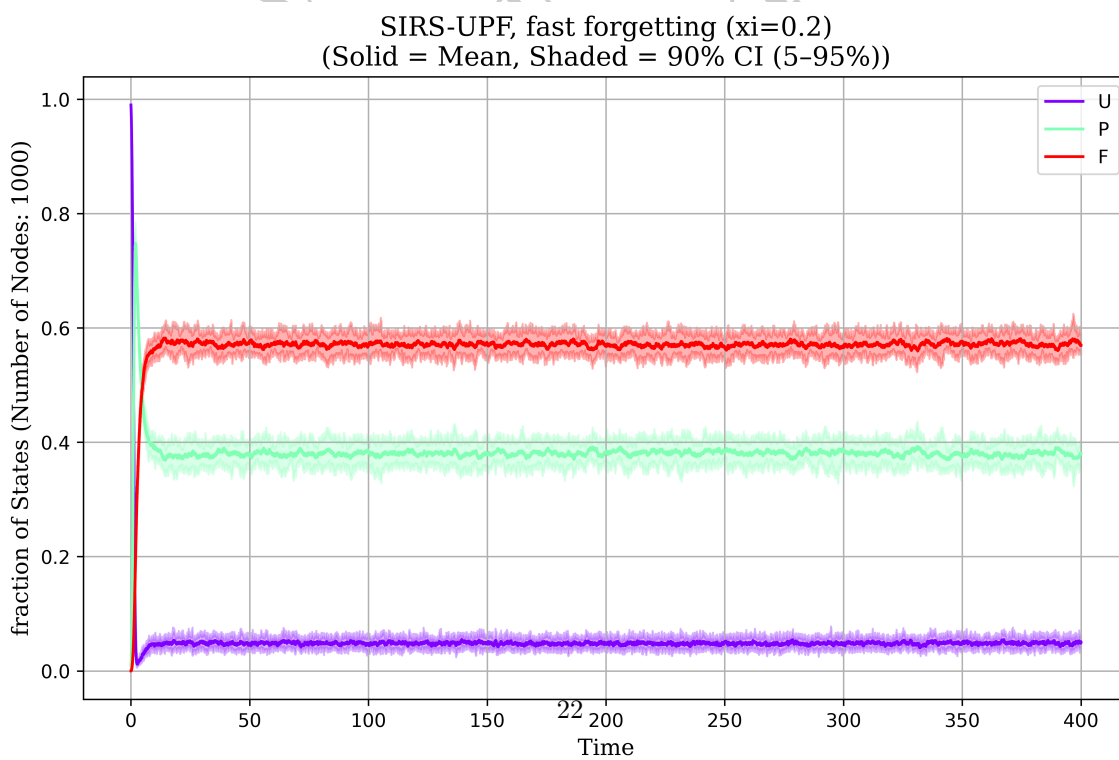


Figure 14: *
results-31.png

Figure 15: Figures: results-21.png and results-31.png

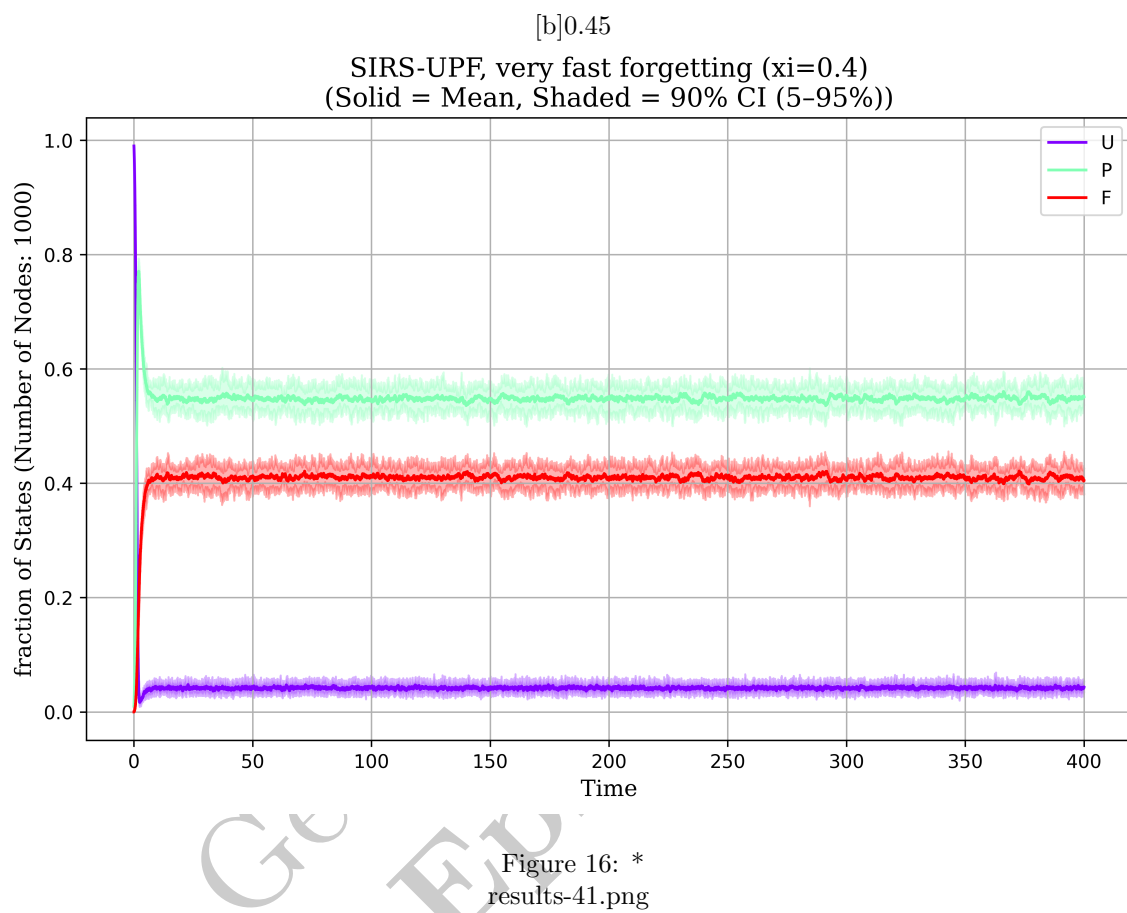


Figure 17: Figures: results-41.png